frontiers | Frontiers in Physics

TYPE Original Research
PUBLISHED 16 September 2025
DOI 10.3389/fphy.2025.1637491

OPEN ACCESS

EDITED BY
Wen-Xiu Ma,
University of South Florida, United States

REVIEWED BY
Saravana Prakash Thirumuruganandham,
SIT Health, Ecuador
Sadique Rehman,
Kanazawa University, Japan

*CORRESPONDENCE
Zhao Li,
lizhao10.26@163.com

RECEIVED 29 May 2025
ACCEPTED 04 August 2025
PUBLISHED 16 September 2025

CITATION
Farooq K, Alshammari FS, Li Z and Hussain E (2025) Soliton dynamics and stability in the Boussinesq equation for shallow water applications.
Front. Phys. 13:1637491.
doi: 10.3389/fphy.2025.1637491

Soliton dynamics and stability in the Boussinesq equation for shallow water applications

Khizar Farooq[1], Fehaid Salem Alshammari[2], Zhao Li[3]* and Ejaz Hussain[4]

[1]Centre for High Energy Physics, University of the Punjab, Lahore, Pakistan, [2]Department of Mathematics and Statistics, College of Science, Imam Mohammad Ibn Saud Islamic University (IMSIU), Riyadh, Saudi Arabia, [3]College of Computer Science, Chengdu University, Chengdu, China, [4]Department of Mathematics, University of the Punjab, Lahore, Pakistan

This manuscript deals with the Fourth-order Boussinesq water wave equation, which is integrable and possesses soliton solutions. Boussinesq water wave equation is a vital tool for investigating nonlinear phenomena in various waves and shallow water phenomena in fluid dynamics, such as diffraction, refraction, weak nonlinearity, and shoaling. Along with fluid dynamics, it is essential in many disciplines of physics, including the transmission of long waves in shallow waters, vibrations in a nonlinear string, acoustics, laser optics, and one-dimensional nonlinear lattice waves. The Generalized Arnous approach, the new Kudryashov method, and the Modified Sub-equation method are applied to this objective. The resultant diverse solutions consist of trigonometric and hyperbolic functions. These approaches generate accurate analytical curves for soliton waves, which comprise kink, bright, and dark waves. The graphical aspects of the produced solutions are investigated using 3*D*-surface graphs, 2*D*-line graphs, and contour and polar plots, in addition to theoretical derivations. This work is novel in its integrated use of three symbolic methods to derive a broad spectrum of exact soliton solutions for the fourth-order Integrated Boussinesq water wave equation, including compound and hybrid waveforms. The inclusion of the graphical visualization, stability analysis, and open source code resources further strengthens its contribution to nonlinear wave modeling.

KEYWORDS

fourth-order boussinesq water wave equation, modified sub-equation method, new Kudryashov method, riccati equation method, solitary wave solutions

1 Introduction

The water wave equation (WWE) was introduced by Boussinesq in 1871 [1].

$$\mathcal{U}_{tt} - \mathcal{U}_{xx} - \sigma(\mathcal{U}^2)_{xx} - \mu\mathcal{U}_{xxxx} = 0. \tag{1.1}$$

This classic Boussinesq equation (BE) defines the shallow-water wave (SWW) solution interaction process. This equation incorporates various waves and shallow water phenomena in fluid dynamics, including shoaling, diffraction, refraction, and weak non-linearity. In addition to fluid dynamics, it is essential in many disciplines of physics, like ions found in waves in plasma, vibrations in non-linear strings, one-dimensional non-linear lattice waves, and the propagation of long waves in shallow water [2]. This study demonstrates the intricate process of how rogue waves are formed and spread in higher dimensions. In addition, we have created a new BE that can be integrated and has varied dimensions [3]. These equations provide a wide range of soliton solutions, contributing to our understanding of wave processes in many physical environments [4]. The focus will be on the fourth-order nonlinear BE.

$$\mathcal{U}_{tt} - \sigma(\mathcal{U}^2)_{xx} - \mu\mathcal{U}_{xxxx} + \nu\mathcal{U}_{xt} - \mathcal{U}_{xx} = 0. \tag{1.2}$$

Here, $\mathcal{U}(x,t)$ represents the surface tension of the water wave, σ denotes the nonlinearity coefficient,μ, and ν are the dispersion coefficients. We see Equation 1.2, originally proposed by Wazwaz and Kaur [4], as completely solvable. Several researchers have investigated different outcomes for nonlinear WWE. For instance, Wang et al. [5] developed advanced Boussinesq-type equations that accurately represent wave dynamics in porous media and apply them to wave propagation in deep water. Fan et al. [6] conducted a study on the use of the widely used $\frac{G'}{G}$-expansion method to analyze the unique solutions of non-linear evolution problems, including the sine-Gordon, Klein–Gordon equation, and BE. Numerous travel solutions were introduced by Kumari cite kumari2020abundant. Jun et al. [7] derived the Backlund transformation and Painleve expansion of Equation 2.1 to employ various solutions. Kumar et al. [8] derived the Lie point symmetry along with the lump and breather solution of Equation 2.1. Understanding wave propagation in shallow seas requires an understanding of the fourth-order nonlinear Boussinesq water wave equation model, which incorporates higher-order nonlinear and dispersive features. This increase enhances the accuracy of wave predictions, making the model particularly helpful for evaluating waves with larger amplitudes and longer wavelengths [9]. This field's applications include coastal engineering and environmental science [10], giving essential insights for coastal development [11], navigation, and disaster prevention [12], including tsunamis and storm surges. The model's complex features allow more realistic modeling of complicated wave interactions, assisting both theoretical research and practical coastal management.

The nonlinear Integrable Boussinesq Water Wave Equation (IBWWE) has emerged as a significant model in various physical phenomena due to its ability to incorporate both nonlinear and dispersive effects with high order accuracy. Its applications span multiple disciplines, including shallow water wave theory [13], nonlinear lattice wave theory [14], coastal engineering [15], and ion-acoustic wave dynamics in plasmas [16]. Due to its high-order structure, the IBWWE provides a refined representation of wave behavior in optical solitons in fiber media and related photonic systems. Given its broad applicability, continued investigation of the IBWWE's soliton structures and analytical properties remains a subject of substantial interest.

Solitary waves [17], or solitons, are self-reinforcing waves that retain their shape while moving at a constant speed. These waves occur in certain nonlinear systems and are solutions to specific nonlinear partial differential equations. A key characteristic of solitary waves is that they do not dissipate or spread out as they travel, unlike typical wave packets that tend to disperse and lose their form over time. Recent developments in mathematical modeling reflect a growing emphasis on accurately characterizing the complex behaviors observed in nature and physical systems. In this context, nonlinear partial differential equations (NLPDEs) offer a robust framework for describing diverse dynamical systems. The development of advanced analytical and computational techniques has facilitated the derivation of exact solutions, enabling the deeper understanding of soliton dynamics, nonlinear wave propagation, and pattern formation. Solitary waves play a key role in several scientific and technical sectors owing to their unusual ability to keep their form and speed across vast distances and via interactions. In physics [18] and engineering [19], solitons are used to simulate stable wave phenomena in nonlinear optics [20], fluid dynamics [21], and plasma physics [22, 23], such as optical pulses in fiber-optic [24] and ion-acoustic waves in space plasmas. They are also significant in biological [25] systems for understanding nerve signal transmission and pattern generation, and in chemistry [26] for characterizing reaction-diffusion processes. In mathematics [27], solitons give insight into nonlinear dynamics [28], chaos theory [29, 30], and integrable systems.

NLPDEs develop as especially significant assets in this scientific quest. Many academics have devoted their efforts to examining distinct NLPDEs to increase their comprehension of the demonstrated behavior in the researched natural phenomena. Recent assessments have involved inquiries into the nonlinear Helmholtz equation [31], complex cubic Nonlinear Schrodinger equation [32], Klein-Fock-Gordon equation [33], Kaup–Newell Model [34], Caudrey–Dodd–Gibbon equation [35]. Studying the single-wave solutions of NLPDEs is crucial for generating improved insights and knowledge of the underlying mechanism and its valuable usage. Therefore, various academics have established novel approaches to investigate these NLPDE replies. Plenty of strong techniques such as EHF technique [36], Darboux transformation [37], exp-function method [38], generalized Kudryashov method [39], extended trial equation method [40], Hirota bilinear method [41], extended Jacobian method [42], extended direct algebraic method [43], NAE method [44], improved extended fan-sub equation method [45], multivariate generalized exponential rational integral function method [46].

Although significant advancements have been made in the computational and symbolic treatment of NLPDEs, analytical exploration of the fourth-order IBWWE, especially in its general form involving dispersive and mixed derivative terms, remains limited. Many of the available methods are limited in scope, only producing restricted forms of solutions. There is a need for comprehensive methods that can produce a border class of exact soliton solutions, including dark, bright, periodic, and compound solitons, while also analyzing the qualitative behavior of stability.

This paper proposes an integrated application of the three advanced solution methods: the Generalized Arnous method [47], the Modified Sub-Equation method [48], and the New Kudryashov method [49], to derive the border spectrum of soliton solutions to the fourth-order IBWWE. Furthermore, a linear stability conducted to assess the robustness of the obtained wave structures. To our knowledge, the combined effects of these three techniques on Equation 1.2, along with he detailed graphical and stability analysis, have not been comprehensively reported in the exciting literature. The Generalized Arnous method is an effective technique for obtaining rational-logarithmic solutions characterized by intricate nonlinear behaviors. The Modified Sub-Equation method utilizes the Riccati type transformations, is particularly suited for the construction of periodic and singular waveforms. The Kudryashov method, recognized for its symbolic strength, is for formulating exact solutions in polynomial-exponential form. Collectively, these methods offer a comprehensive analytical framework to yield a richer and more diverse set of analytical solutions, including mixed and compound solutions.

The article is summarized as follows: Section 2 outlines the mathematical analysis required to transform the nonlinear partial differential problem into an ordinary differential equation. Section 3 examines the Generalized Arnous method, its applications, and includes graphical representations. Section 4 highlights the application of the Modified Sub-Equation method. Section 5 delves into the mathematical framework and applications of the New Kudryashov method. Section 6 focuses on the stability analysis. Section 7 discusses the graphical representation of solutions, and finally, Section 8 concludes the study.

2 Formulation of governing model

Consider a general NLPDE has the following form [27, 50]:

$$Y(\mathcal{U},\mathcal{U}_t,\mathcal{U}_x,\mathcal{U}_{xt},\mathcal{U}_{xx},\ldots)=0. \tag{2.1}$$

Its NODE will be

$$P(\Xi,\Xi',\Xi'',\ldots)=0. \tag{2.2}$$

Consider the traveling wave ansatz solution to simplify the NLPDEs into NLODEs [51, 52].

$$\mathcal{U}(x,t)=\Xi(\xi);\xi=\omega x-\eta t. \tag{2.3}$$

Here, ω represents the wave number, and η denotes the wave speed.

The fourth-order nonlinear differential Boussinesq water wave equation is given as [53]:

$$\Xi_{tt}-\sigma(\Xi^2)_{xx}-\mu\Xi_{xxxx}+\nu\Xi_{xt}-\Xi_{xx}=0 \tag{2.4}$$

Now by using Equation 2.3 in Equation 2.4 we get:

$$\mu\omega^4\Xi^{(4)}-\Xi''\left(-\nu\omega\eta-\omega^2+\eta^2\right)+2\sigma\omega^2\Xi\Xi''+2\sigma\omega^2(\Xi')^2=0. \tag{2.5}$$

After integrating Equation 2.5 twice w. r.t ξ we get [54, 55]:

$$\sigma\omega^2\Xi^2+\mu\omega^4\Xi''-\Xi\left(-\nu\omega\eta-\omega^2+\eta^2\right)=0. \tag{2.6}$$

3 The Generalized Arnous methods

The basic steps of the generalized Arnous (GA) method are as follows [47].

Step 1: The (GA) method provides the solution of Equation 2.3 as follows:

$$\Xi(\xi)=\alpha_0+\sum_{1=1}^{N}\frac{\alpha_i+\beta_i g'(\xi)^i}{g(\xi)^i}. \tag{3.1}$$

where α_0, α_i, β_i (for i = 1, 2, …, N) are real constants with condition $\alpha_N^2+\beta_N^2\neq 0$, and the function $g(\xi)$ verified the relation

$$[g'(\xi)]^2=[g(\xi)^2-\rho]\ln[\gamma]. \tag{3.2}$$

with,

$$g^{(n)}(\xi)=\begin{cases} g(\xi)\ln(\gamma)^n, & \text{if } n \text{ is even,}\\ g'(\xi)\ln(\gamma)^{n-1}, & \text{if } n \text{ is odd,}\end{cases} \tag{3.3}$$

where $n\geq 2$, and $0<\gamma\neq 1$. Equation 3.2 has solutions of the form:

$$g(\xi)=A\ln(\gamma)\gamma^{\xi}+\frac{\rho}{4A\ln}(\gamma)\gamma^{\xi}. \tag{3.4}$$

Here ρ, A, and γ are real constants.

Step 2: By balancing the non-linear term with the highest order derivative in Equation 2.6, the positive integer N is determined for Equation 3.1.

Step 3: After inserting Equations 3.1-3.3 in Equation 2.6 and since $g^i(\xi)\neq 0$, as a result of this substitution we get a polynomial of $\frac{1}{g(\xi)}\left(\frac{g'(\xi)}{g(\xi)}\right)$. Equivalently, setting all terms with the same power equal to zero. Then, by solving this set of non-linear algebraic systems and with the help of Equation 3.2 and Equation 2.3, the solutions of Equation 1.2 may be determined.

3.1 Solutions by Generalized Arnous Method

To find the exact solution of Equation 2.6, first we find the value of positive integer $N=2$ and plug the value of N into Equation 3.1 then Equation 3.1 will become as follows:

$$\Xi(\xi)=\alpha_0+\frac{\alpha_1}{g(\xi)}+\frac{\beta_1 g'(\xi)}{g(\xi)}+\frac{\alpha_2}{g(\xi)^2}+\frac{\beta_2(g''(\xi))^2}{g(\xi)^2}. \tag{3.5}$$

By inserting Equation 3.5 into Equation 2.6 together with Equation 3.2 and Equation 2.3, we have a polynomial in terms of $\frac{1}{g(\xi)}\left(\frac{g'(\xi)}{g(\xi)}\right)$. This creates a system of algebraic equations when we aggregate all terms of the same power and put them equal to zero. The values of unknown constants are obtained.

Set 1.

$$\begin{aligned}&\alpha_0=\beta_2\left(-\ln^2(\gamma)\right),\alpha_1=0,\beta_1=0,\\ &\eta=\frac{1}{2}\left(-\sqrt{\omega^2\left(-16\mu\omega^2\ln^2(\gamma)+\nu^2+4\right)}-\nu\omega\right),\\ &\alpha_2=\frac{\rho\ln^2(\gamma)\left(\beta_2\sigma+6\mu\omega^2\right)}{\sigma}.\end{aligned} \tag{3.6}$$

By putting set 1 in Equation 3.5 we obtained the exact solution as follows:

$$\Xi_1(\xi)=\left[\frac{\rho\ln^2(\gamma)\left(\beta_2\lambda+6\mu\omega^2\right)}{\lambda\left(\frac{\rho\gamma^{-\xi}}{4A\ln(\gamma)}+A\gamma^{\xi}\ln(\gamma)\right)^2}+\frac{\beta_2\left(A\gamma^{\xi}\ln^2(\gamma)-\frac{\rho\gamma^{-\xi}}{4A}\right)^2}{\left(\frac{\rho\gamma^{-\xi}}{4A\ln(\gamma)+A\gamma^{\xi}\ln}(\gamma)\right)^2}-\beta_2\ln^2(\gamma)\right]. \tag{3.7}$$

Set 2.

$$\alpha_0 = -\frac{\ln^2(\gamma)(\beta_2\lambda + 4\mu\omega^2)}{\lambda}, \alpha_1 = 0, \beta_1 = 0, \alpha_2 = \frac{\rho\ln^2(\gamma)(\beta_2\lambda + 6\mu\omega^2)}{\lambda},$$
$$v = \frac{4\mu\omega^4\ln^2(\gamma) - \eta^2 + \omega^2}{\eta\omega}. \tag{3.8}$$

By putting set 1 in Equation 3.5 we obtained the exact solution as follows:

$$\Xi_2(\xi) = \left[\frac{\rho\ln^2(\gamma)(\beta_2\lambda + 6\mu\omega^2)}{\lambda\left(\frac{\rho\gamma^{-\xi}}{4A\ln}(\gamma) + A\gamma^{\xi}\ln(\gamma)\right)^2} + \frac{\beta_2\left(A\gamma^{\xi}\ln^2(\gamma) - \frac{\rho\gamma^{-\xi}}{4A}\right)^2}{\left(\frac{\rho\gamma^{-\xi}}{4A\ln}(\gamma) + A\gamma^{\xi}\ln(\gamma)\right)^2} - \frac{\ln^2(\gamma)(\beta_2\lambda + 4\mu\omega^2)}{\lambda}\right]. \tag{3.9}$$

4 The modified sub-equation methods

The basic steps of the Modified sub-equation (MSE) method are as follows [56].

Step 1: The (MSE) method provides the solution of Equation 2.3 as follows:

$$\Xi(\xi) = c_0 + \sum_{j=1}^{N} c_j g_j(\xi). \tag{4.1}$$

c_0, c_j (for j = 1, 2, …, N) are non zero constants, with the condition $c_N \neq 0$, and the function $g(\xi)$ in Equation 4.1 satisfied the relation:

$$g'(\xi) = \sqrt{\lambda_2 g^4(\xi) + \lambda_1 g^2(\xi) + \lambda_0}. \tag{4.2}$$

Here λ_0, λ_1, and $\lambda_2 \neq 0$ are real constants. The answer to Equation 4.2 as follows.

Case 1: When $\lambda_0 = 0, \lambda_1 > 0$, and $\lambda_2 \neq 0$ then,

$$g^{01}(\xi) = \pm\sqrt{-\frac{\lambda_1}{\lambda_2}}\operatorname{sech}\left[\sqrt{\lambda_1}\xi + \rho\right]. \tag{4.3}$$

$$g^{02}(\xi) = \pm\sqrt{\frac{\lambda_1}{\lambda_2}}\operatorname{csch}\left[\sqrt{\lambda_1}\xi + \rho\right]. \tag{4.4}$$

Case 2: In case of constants A_1 and A_2 $\lambda_0 = 0, \lambda_1 > 0$, and $\lambda_2 = \pm 4A_1A_2$ then,

$$g^{03}(\xi) = \pm\frac{4\sqrt{\lambda_1}A_1}{(4A_1^2 - \lambda_2)\cosh\left(\sqrt{\lambda_1}(\xi + \rho)\right) + (4A_1^2 + \lambda_2)\sinh\left(\sqrt{\lambda_1}(\xi + \rho)\right)}. \tag{4.5}$$

Case 3: Consider $\lambda_0 = \frac{\lambda_1^2}{4\lambda_2}, \lambda_1 < 0$, and $\lambda_2 > 0$ then,

$$g^{04}(\xi) = \pm\sqrt{-\frac{\lambda_1}{2\lambda_2}}\tanh\left[\sqrt{\frac{-\lambda_1}{2}}\xi + \rho\right]. \tag{4.6}$$

$$g^{05}(\xi) = \pm\sqrt{-\frac{\lambda_1}{2\lambda_2}}\coth\left[\sqrt{\frac{-\lambda_1}{2}}\xi + \rho\right]. \tag{4.7}$$

$$g^{06}(\xi) = \pm\sqrt{-\frac{\lambda_1}{2\lambda_2}}\left[\tanh\left(\sqrt{-2\lambda_1}\xi + \rho\right) + \imath\operatorname{sech}\left(\sqrt{-2\lambda_1}\xi + \rho\right)\right]. \tag{4.8}$$

$$g^{07}(\xi) = \pm\sqrt{-\frac{\lambda_1}{2\lambda_2}}\left[\tanh\left(\sqrt{-2\lambda_1}\xi + \rho\right) + \imath\operatorname{sech}\left(\sqrt{-2\lambda_1}\xi + \rho\right)\right]^{-1}. \tag{4.9}$$

Case 4: When $\lambda_0 = 0, \lambda_1 < 0$, and $\lambda_2 \neq 0$ then,

$$g^{08}(\xi) = \pm\sqrt{-\frac{\lambda_1}{2\lambda_2}}\sec\left[\sqrt{-\lambda_1}\xi + \rho\right]. \tag{4.10}$$

$$g^{09}(\xi) = \pm\sqrt{-\frac{\lambda_1}{2\lambda_2}}\csc\left[\sqrt{-\lambda_1}\xi + \rho\right]. \tag{4.11}$$

Case 5: Consider $\lambda_0 = \frac{\lambda_1^2}{4\lambda_2}, \lambda_1 > 0$, and $\lambda_2 > 0$ then,

$$g^{10}(\xi) = \pm\sqrt{\frac{\lambda_1}{2\lambda_2}}\tan\left[\sqrt{\frac{\lambda_1}{2}}\xi + \rho\right]. \tag{4.12}$$

$$g^{11}(\xi) = \pm\sqrt{\frac{\lambda_1}{2\lambda_2}}\cot\left[\sqrt{\frac{\lambda_1}{2}}\xi + \rho\right]. \tag{4.13}$$

$$g^{12}(\xi) = \pm\sqrt{\frac{\lambda_1}{2\lambda_2}}\left[\tan\left(\sqrt{2\lambda_1}\xi + \rho\right) + \sec\left(\sqrt{2\lambda_1}\xi + \rho\right)\right]. \tag{4.14}$$

$$g^{13}(\xi) = \pm\sqrt{\frac{\lambda_1}{2\lambda_2}}\left[\tan\left(\sqrt{2\lambda_1}\xi + \rho\right) + \sec\left(\sqrt{2\lambda_1}\xi + \rho\right)\right]^{-1}. \tag{4.15}$$

Case 6: If $\lambda_0 = 0, \lambda_1 > 0$ then,

$$g^{14}(\xi) = \pm\frac{4\lambda_1 e^{\sqrt{\lambda_1}\xi + \rho}}{e^{2\sqrt{\lambda_1}\xi + \rho} - 4\lambda_1\lambda_2}. \tag{4.16}$$

$$g^{15}(\xi) = \pm\frac{4\lambda_1 e^{\sqrt{\lambda_1}\xi + \rho}}{1 - 4\lambda_1\lambda_2 e^{2\sqrt{\lambda_1}\xi + \rho}}. \tag{4.17}$$

Case 7: When $\lambda_0 = \lambda_1 = 0, \lambda_2 > 0$ then,

$$g^{16}(\xi) = \pm\frac{1}{\sqrt{\lambda_2}\xi + \rho}. \tag{4.18}$$

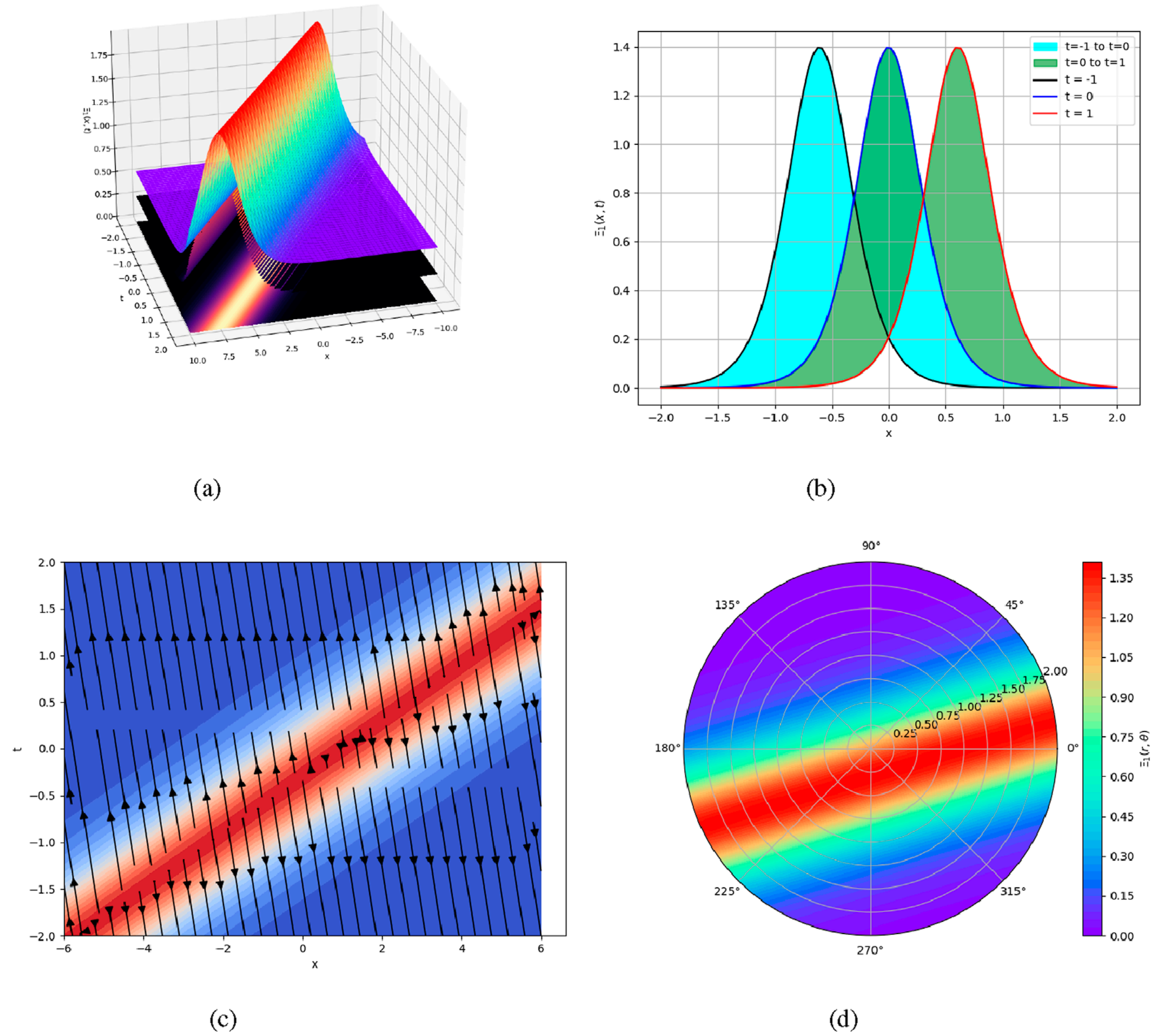

FIGURE 1
Graphical visualization of derived solution of Equation 3.7 gives bright soliton such as **(a)** 3D surface, **(b)** 2D surface, **(c)** Streamline Plot **(d)** Polar Polt, of $\Xi_{01}(x,t)$: $\rho = 1$, $\theta = 0.2$, $\mu = 1$, $\omega = 0.3$, $\beta_2 = 1$, $\sigma = 1$, $\eta = 1$, $A = 0.5$.

Case 8: If $\lambda_0 = \lambda_1 = 0, \lambda_2 > 0$ then,

$$g^{17}(\xi) = \pm \frac{\iota}{\sqrt{-\lambda_2 \xi + \rho}}. \tag{4.19}$$

Step 2: By balancing the non-linear term with the highest order derivative in Equation 2.6, the positive integer N is determined for Equation 4.1.

Step 3: After inserting Equations 4.1–4.2 in Equation 2.6 and since $g^i(\xi) \neq 0$, for (i = 1,2,3,..., N), as a result of this substitution we get a polynomial of $g^i(\xi)$. Equivalently, setting all terms with the same power equal to zero. Then by solving this set of non-linear algebraic systems and with the help of Equation 4.2 and Equation 2.3, the solutions of Equation 1.2 may be determined.

4.1 Solution by the modified sub-equation method

To find the exact solution of Equation 2.6, first we find value of positive integer $N = 2$ and plugging the value of N in to Equation 4.1 then Equation 4.1 will become as follows:

$$\Xi(\xi) = c_0 + c_1 g(\xi) + c_2 g(\xi)^2. \tag{4.20}$$

By inserting Equation 4.20 into Equation 1.2 together with Equation 2.3 and Equation 4.2, we have a polynomial in terms of $g^i(\xi)$. This creates a system of algebraic equations when we aggregate

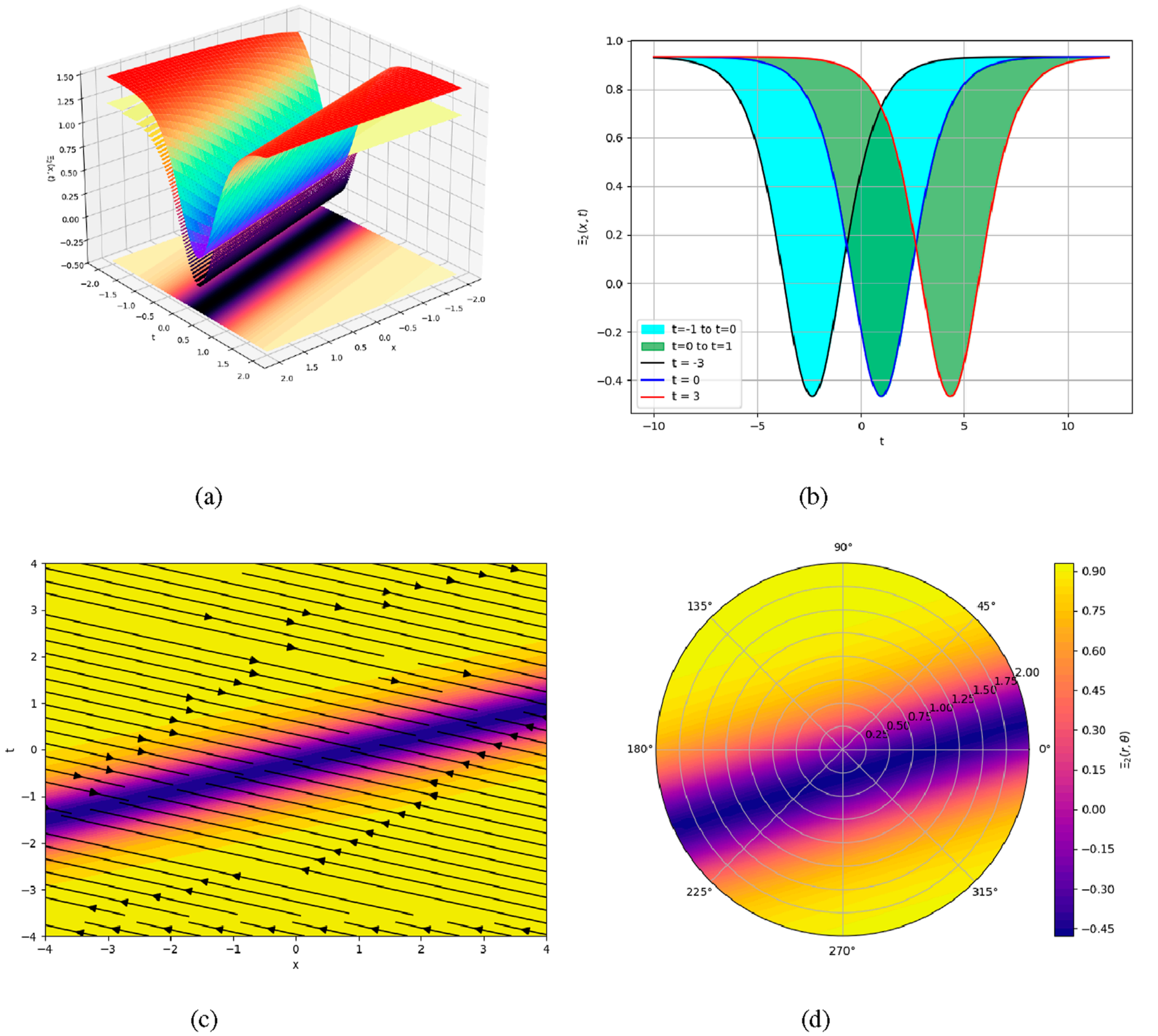

FIGURE 2
Graphical visualization of derived solution of Equation 3.9 gives dark soliton such as **(a)** 3D surface, **(b)** 2D surface, **(c)** Streamline Plot **(d)** Polar Polt, of $\Xi_{02}(x,t)$: $\rho = 1$, $\theta = 0.2$, $\mu = 1$, $\omega = 0.3$, $\beta_2 = 1$, $\sigma = 1$, $\eta = 1$, $A = 0.5$.

all terms of the same power and put them equal to zero. The values of unknown constants are obtained.

Set 1:

$$v = \frac{-\left(4\mu\omega^4\lambda_1 + 4\omega^4\left(-\lambda_1 + \sqrt{-3\lambda_0\lambda_2 + \lambda_1^2}\right)\mu - \eta^2 + \omega^2\right)}{\eta\omega},$$
$$c_0 = \frac{2\left(-\lambda_1 + \sqrt{-3\lambda_0\lambda_2 + \lambda_1^2}\right)\omega^2\mu}{\lambda} \tag{4.21}$$
$$c_1 = 0, c_2 = -\frac{6\mu\omega^2\lambda_2}{\lambda}.$$

By putting Set 1 in Equation 4.20 we get the exact solutions as follows.

Case 1: When $\lambda_0 = 0, \lambda_1 > 0$, and $\lambda_2 \neq 0$ then,

$$\Xi_{01}(x,t) = \frac{2\left(-\lambda_1 + \sqrt{-3\lambda_0\lambda_2 + \lambda_1^2}\right)\omega^2\mu}{\sigma} + \frac{6\mu\omega^2\lambda_1 \operatorname{sech}\left(\sqrt{\lambda_1}\,\xi + \rho\right)^2}{\sigma}. \tag{4.22}$$

$$\Xi_{02}(x,t) = \frac{2\left(-\lambda_1 + \sqrt{-3\lambda_0\lambda_2 + \lambda_1^2}\right)\omega^2\mu}{\sigma} - \frac{6\mu\omega^2\lambda_1 \operatorname{csch}\left(\sqrt{\lambda_1}\,\xi + \rho\right)^2}{\sigma}. \tag{4.23}$$

Case 2: In case of constants A_1 and A_2, $\lambda_0 = 0, \lambda_1 > 0$, and $\lambda_2 = \pm 4A_1 A_2$ then,

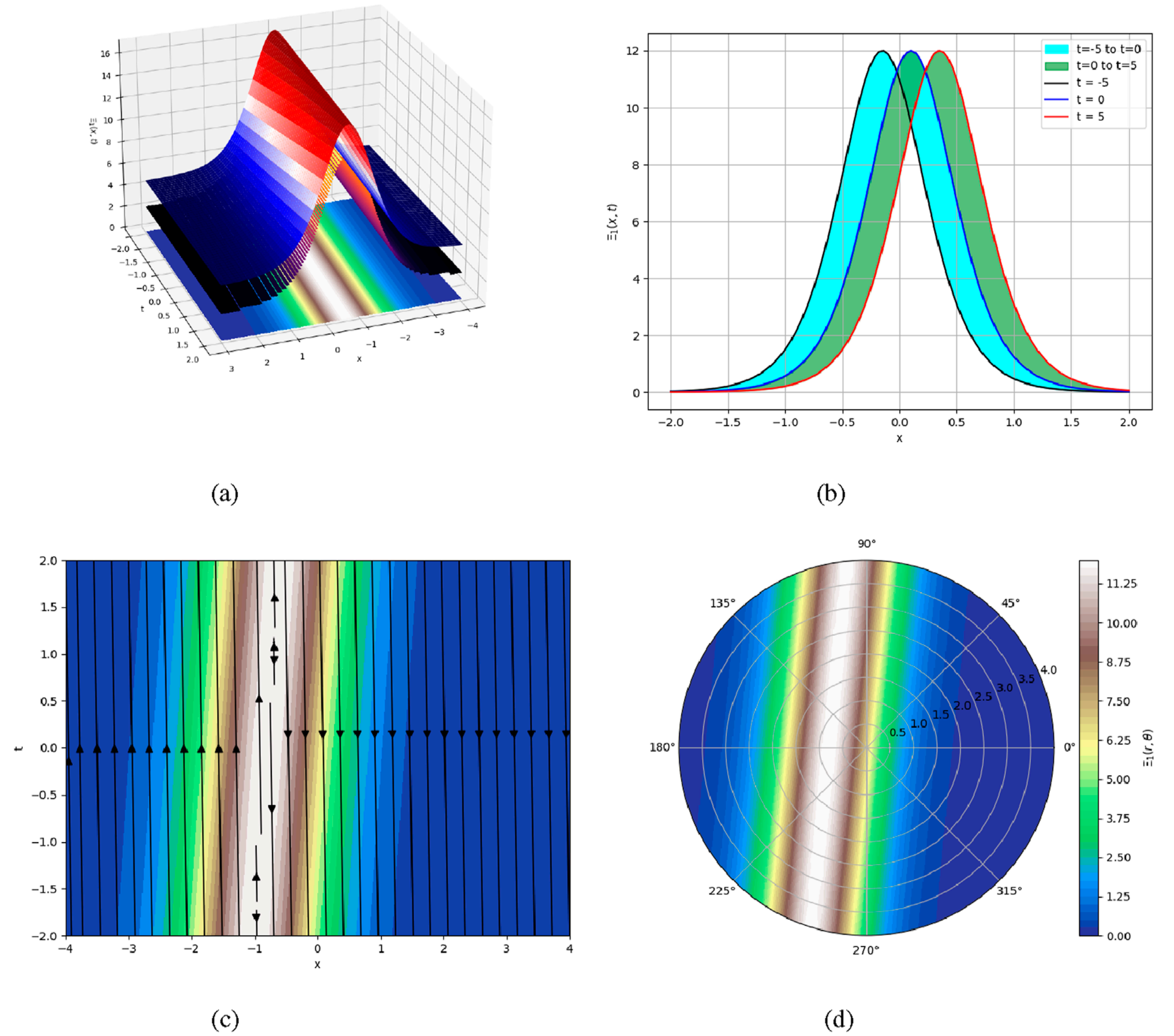

FIGURE 3
Graphical visualization of derived solution of Equation 4.22 gives bright soliton such as **(a)** 3D surface, **(b)** 2D surface, **(c)** Streamline Plot **(d)** Polar Plot, of $\Xi_{01}(x,t)$: $\lambda_0 = 0, \quad \lambda_1 = 1, \quad \lambda_2 = 2, \quad \mu = 2, \quad \sigma = 1, \quad \rho = 0.8, \quad \eta = 0.5, \quad \omega = 1, \quad \nu = -8.$

$$\Xi_{03}(x,t) = -\frac{96\mu\omega^2\lambda_2\lambda_1 A_1^2}{\sigma\left((4A_1^2-\lambda_2)\cosh\left(\sqrt{\lambda_1}(\xi+\rho)\right)+(4A_1^2+\lambda_2)\sinh\left(\sqrt{\lambda_1}(\xi+\rho)\right)\right)^2} + \frac{2\left(-\lambda_1+\sqrt{-3\lambda_0\lambda_2+\lambda_1^2}\right)\omega^2\mu}{\sigma}. \tag{4.24}$$

Case 3: Consider $\lambda_0 = \frac{\lambda_1^2}{4\lambda_2}, \lambda_1 < 0$, and $\lambda_2 > 0$ then,

$$\Xi_{04}(x,t) = \frac{2\left(-\lambda_1+\sqrt{-3\lambda_0\lambda_2+\lambda_1^2}\right)\omega^2\mu}{\sigma} + \frac{3\mu\omega^2\lambda_1\tanh\left(\frac{\sqrt{-2\lambda_1}\,\xi}{2}+\rho\right)^2}{\sigma}. \tag{4.25}$$

$$\Xi_{05}(x,t) = \frac{2\left(-\lambda_1+\sqrt{-3\lambda_0\lambda_2+\lambda_1^2}\right)\omega^2\mu}{\sigma} + \frac{3\mu\omega^2\lambda_1\coth\left(\frac{\sqrt{-2\lambda_1}\,\xi}{2}+\rho\right)^2}{\sigma}. \tag{4.26}$$

$$\Xi_{06}(x,t) = \frac{2\left(-\lambda_1+\sqrt{-3\lambda_0\lambda_2+\lambda_1^2}\right)\omega^2\mu}{\sigma} + \frac{3\mu\omega^2\lambda_1\left(\tanh\left(\sqrt{-2\lambda_1}\,\xi+\rho\right)+\mathrm{I}\,\mathrm{sech}\left(\sqrt{-2\lambda_1}\,\xi+\rho\right)\right)^2}{\sigma}. \tag{4.27}$$

$$\Xi_{07}(x,t) = \frac{2\left(-\lambda_1+\sqrt{-3\lambda_0\lambda_2+\lambda_1^2}\right)\omega^2\mu}{\sigma} + \frac{3\mu\omega^2\lambda_1}{\sigma\left(\tanh\left(\sqrt{-2\lambda_1}\,\xi+\rho\right)+\mathrm{I}\,\mathrm{sech}\left(\sqrt{-2\lambda_1}\,\xi+\rho\right)\right)^2}. \tag{4.28}$$

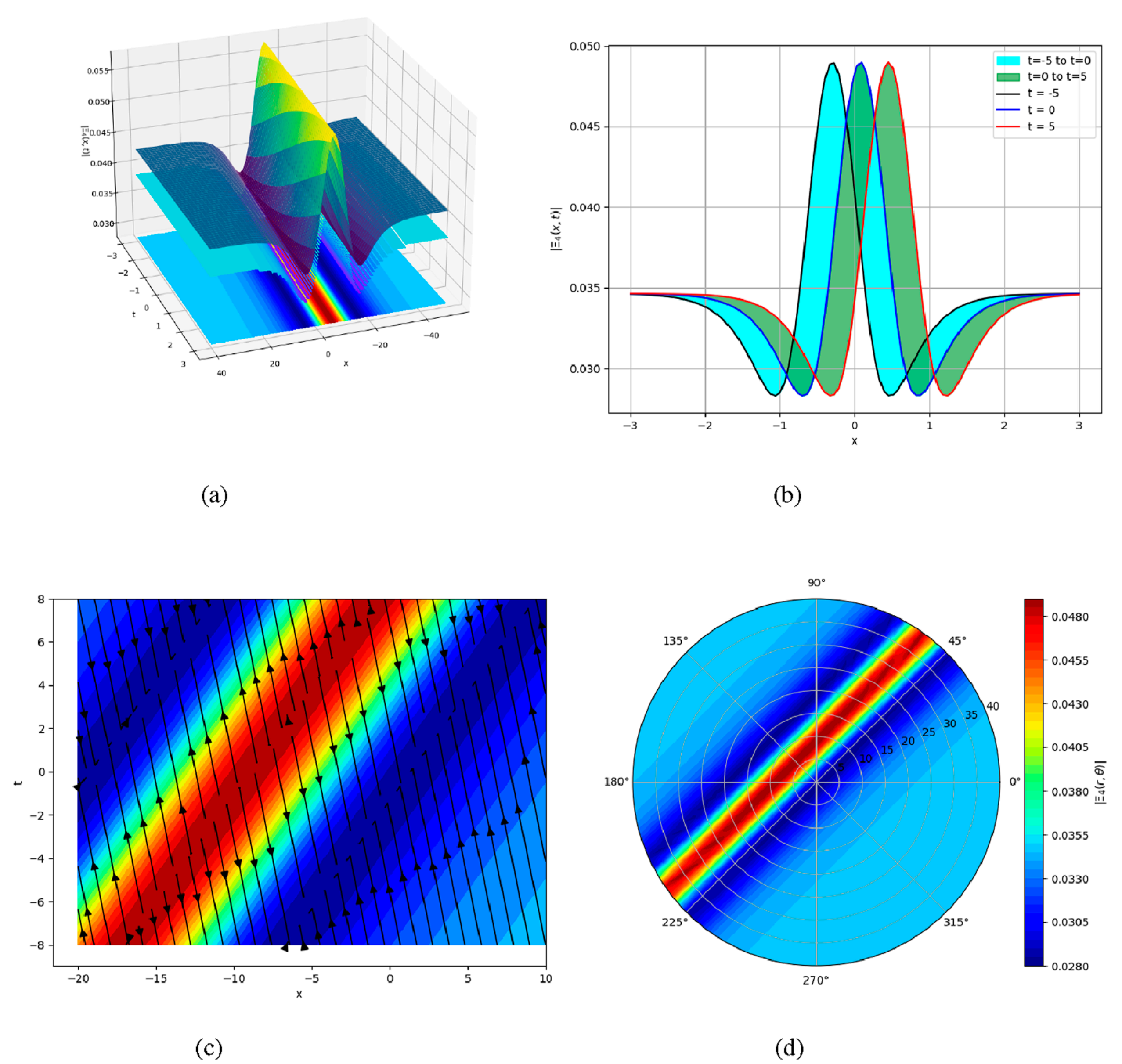

FIGURE 4
Graphical visualization of derived solution of Equation 4.25 gives dark-bright soliton such as **(a)** 3D surface, **(b)** 2D surface, **(c)** Streamline Plot **(d)** Polar Plot, of $|\Xi_{04}(x,t)|$: $\lambda_0 = 0.005$, $\lambda_1 = -0.1$, $\lambda_2 = 0.5$, $\mu = 2$, $\sigma = -2.5$, $\rho = 1$, $\eta = 0.5$, $\omega = 0.5$, $\nu = 0.56$.

Case 4: When $\lambda_0 = 0, \lambda_1 < 0$, and $\lambda_2 \neq 0$ then,

$$\Xi_{08}(x,t) = \frac{2\left(-\lambda_1 + \sqrt{-3\lambda_0\lambda_2 + \lambda_1^2}\right)\omega^2\mu}{\sigma} + \frac{3\mu\,\omega^2\lambda_1\,\sec\left(\sqrt{-\lambda_1}\,\xi + \rho\right)^2}{\sigma}. \tag{4.29}$$

$$\Xi_{09}(x,t) = \frac{2\left(-\lambda_1 + \sqrt{-3\lambda_0\lambda_2 + \lambda_1^2}\right)\omega^2\mu}{\sigma} + \frac{3\mu\,\omega^2\lambda_1\,\csc\left(\sqrt{-\lambda_1}\,\xi + \rho\right)^2}{\sigma}. \tag{4.30}$$

Case 5: Consider $\lambda_0 = \frac{\lambda_1^2}{4\lambda_2}, \lambda_1 > 0$, and $\lambda_2 > 0$ then,

$$\Xi_{10}(x,t) = \frac{2\left(-\lambda_1 + \sqrt{-3\lambda_0\lambda_2 + \lambda_1^2}\right)\omega^2\mu}{\sigma} - \frac{3\mu\,\omega^2\lambda_1\,\tan\left(\frac{\sqrt{2}\sqrt{\lambda_1}\,\xi}{2} + \rho\right)^2}{\sigma}. \tag{4.31}$$

$$\Xi_{11}(x,t) = \frac{2\left(-\lambda_1 + \sqrt{-3\lambda_0\lambda_2 + \lambda_1^2}\right)\omega^2\mu}{\sigma} - \frac{3\mu\,\omega^2\lambda_1\,\cot\left(\frac{\sqrt{2}\sqrt{\lambda_1}\,\xi}{2} + \rho\right)^2}{\sigma}. \tag{4.32}$$

$$\Xi_{12}(x,t) = \frac{2\left(-\lambda_1 + \sqrt{-3\lambda_0\lambda_2 + \lambda_1^2}\right)\omega^2\mu}{\sigma} - \frac{3\mu\,\omega^2\lambda_1\left(\tan\left(\sqrt{2}\sqrt{\lambda_1}\,\xi + \rho\right) + \sec\left(\sqrt{2}\sqrt{\lambda_1}\,\xi + \rho\right)\right)^2}{\sigma}. \tag{4.33}$$

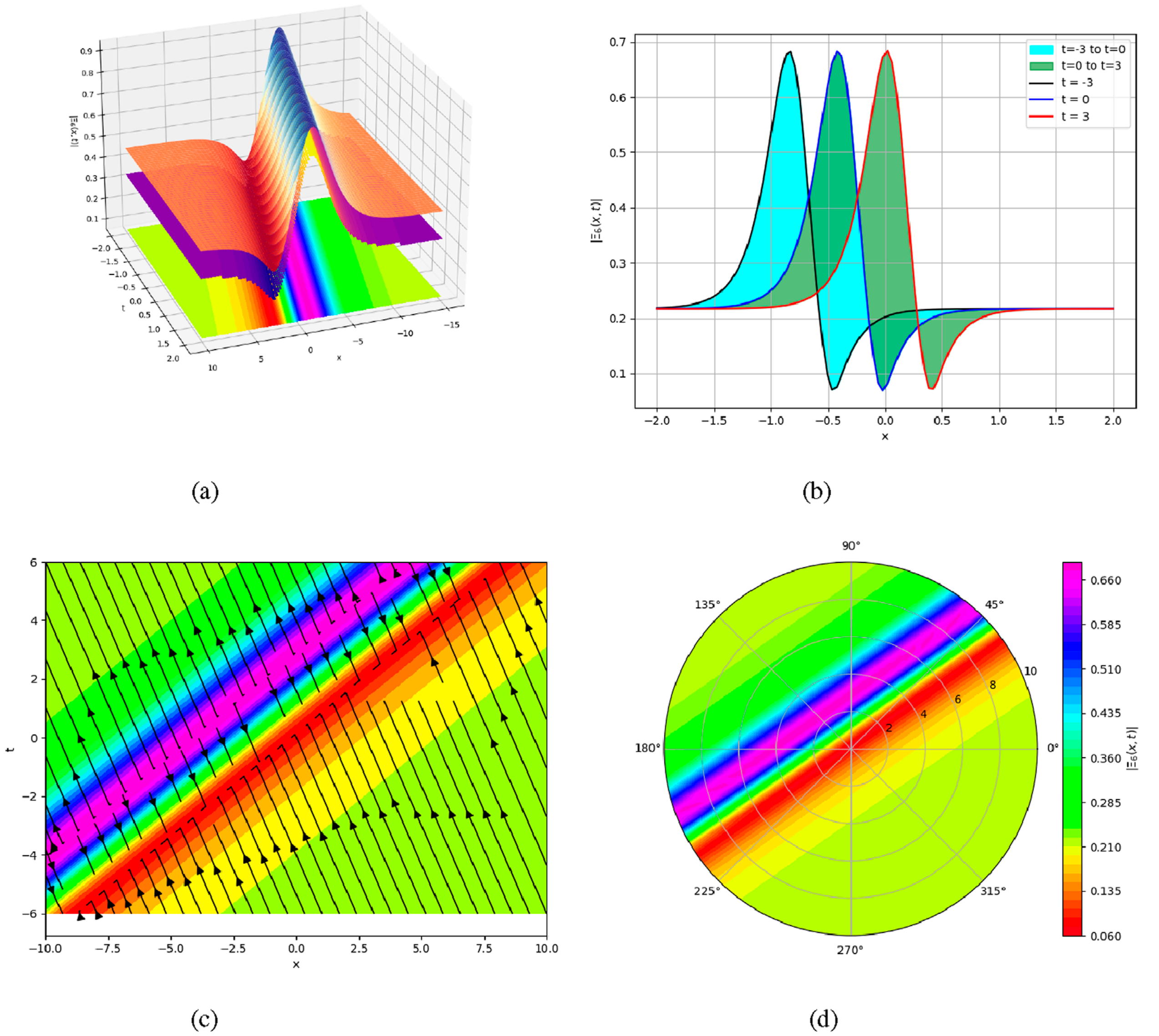

FIGURE 5
Graphical visualization of derived solution of Equation 4.27 gives bright-dark soliton such as **(a)** 3D surface, **(b)** 2D surface, **(c)** Streamline Plot **(d)** Polar Plot, of $|\Xi_{06}(x,t)|$: $\lambda_0 = 0.001$, $\lambda_1 = -0.08$, $\lambda_2 = 1.2$, $\mu = 2$, $\sigma = -2.5$, $\rho = 2$, $\eta = 2$, $\omega = 1.4$, $\nu = 0.72 - 0.65I$.

$$\Xi_{13}(x,t) = \frac{2\left(-\lambda_1 + \sqrt{-3\lambda_0\lambda_2 + \lambda_1^2}\right)\omega^2\mu}{\sigma} - \frac{3\mu\omega^2\lambda_1}{\sigma\left(\tan\left(\sqrt{2}\sqrt{\lambda_1}\xi + \rho\right) + \sec\left(\sqrt{2}\sqrt{\lambda_1}\xi + \rho\right)\right)^2}. \tag{4.34}$$

Case 6: If $\lambda_0 = 0, \lambda_1 > 0$ then,

$$\Xi_{14}(x,t) = \pm\frac{4\lambda_1 e^{\sqrt{\lambda_1}\xi+\rho}}{e^{2\sqrt{\lambda_1}\xi+\rho} - 4\lambda_1\lambda_2}. \tag{4.35}$$

$$\Xi_{15}(x,t) = \pm\frac{4\lambda_1 e^{\sqrt{\lambda_1}\xi+\rho}}{1 - 4\lambda_1\lambda_2 e^{2\sqrt{\lambda_1}\xi+\rho}}. \tag{4.36}$$

Case 7: When $\lambda_0 = \lambda_1 = 0, \lambda_2 > 0$ then,

$$\Xi_{16}(x,t) = \frac{2\left(-\lambda_1 + \sqrt{-3\lambda_0\lambda_2 + \lambda_1^2}\right)\omega^2\mu}{\sigma} - \frac{6\mu\omega^2\lambda_2}{\sigma\left(\sqrt{\lambda_2}\xi + \rho\right)^2}. \tag{4.37}$$

Case 8: If $\lambda_0 = \lambda_1 = 0, \lambda_2 > 0$ then,

$$\Xi_{17}(x,t) = \frac{2\left(-\lambda_1 + \sqrt{-3\lambda_0\lambda_2 + \lambda_1^2}\right)\omega^2\mu}{\sigma} + \frac{6\mu\omega^2\lambda_2}{\sigma\left(\sqrt{-\lambda_2}\xi + \rho\right)^2}. \tag{4.38}$$

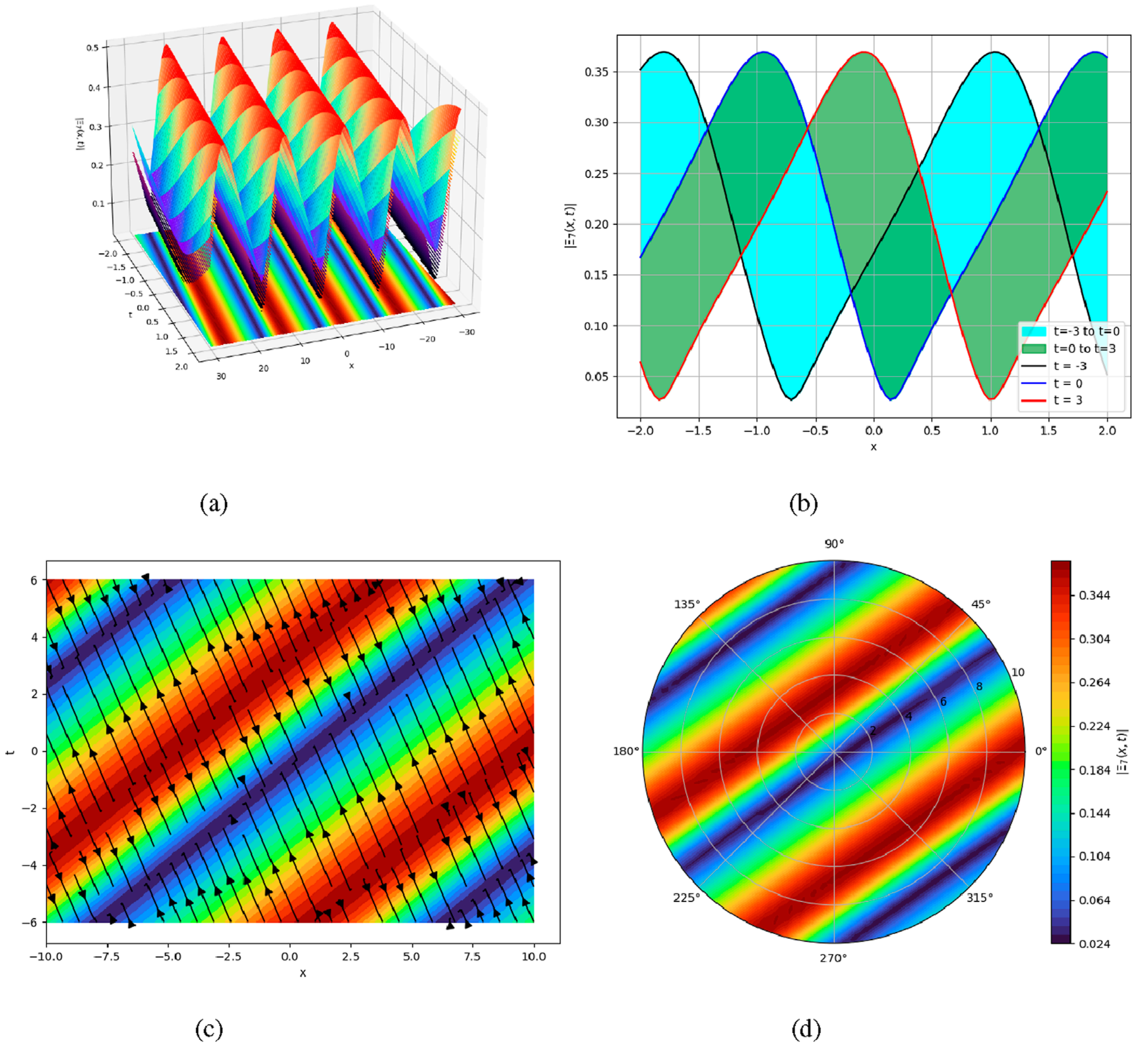

FIGURE 6
Graphical visualization of derived solution of Equation 4.28 gives periodic soliton such as **(a)** 3D surface, **(b)** 2D surface, **(c)** Streamline Plot **(d)** Polar Plot, of $|\Xi_{07}(x,t)|$: $\lambda_0 = 0.0006$, $\lambda_1 = 0.05$, $\lambda_2 = 1$, $\mu = 1$, $\sigma = 1$, $\rho = 1$, $\eta = 2$, $\omega = 1.4$, $v = 0.72 - 0.19I$.

5 The New Kudryashov methods

Here are some important steps of the new Kudryashov method (NK).

Step 1: The NK method provides the solution of Equation 2.6 as:

$$\Xi(\xi) = c_0 + \sum_{i=1}^{N} \left[l_i g^i(\xi) \right]. \tag{5.1}$$

where the coefficients l_i for i = 0, 1, 2,…, N are constants to be determined such that $l_N \neq 0$, and $g(\xi) = \frac{1}{aB^{\delta\xi} + bB^{-\delta\xi}}$ is the solution of the following non-linear ODE:

$$g'(\xi)^2 = (\delta \ln(B) g(\xi))^2 \left(1 - 4abg^2(\xi)\right). \tag{5.2}$$

$$g''(\xi) = \left(\delta^2 \ln(B)^2 g(\xi)\right)\left(1 - 8abg^2(\xi)\right). \tag{5.3}$$

here constants a, b, δ, and B are all non-zero, with $B > 0$ and $B \neq 1$.

Step 2: Using the homogeneous balance principle, we may get the positive integer N by balancing the highest-order derivative and nonlinear variables in Equation 2.3.

Step 3: After inserting Equation 5.1 into Equation 2.6 and recognizing that $g(\xi) \neq 0$ we set all coefficients of $g^i(\xi)$ to zero. After that, we get particular values for a, b, and the c_i's by solving the resultant non-linear algebraic system. By plugging the values back into Equation 5.1 and applying the transformation of Equation 2.3, we may get a solution for Equation 1.2.

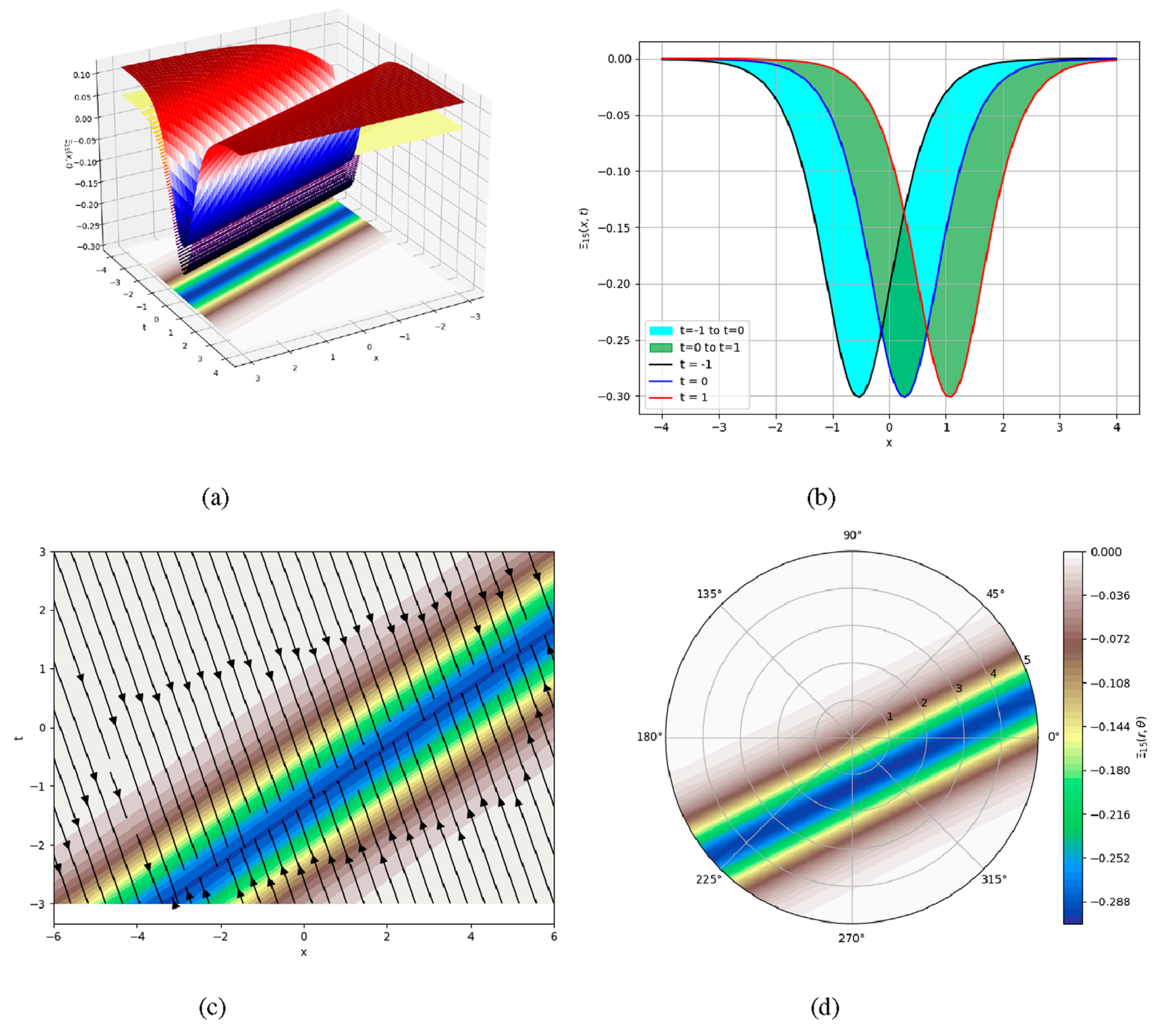

FIGURE 7
Graphical visualization of derived solution of Equation 4.38 gives dark soliton such as **(a)** 3D surface, **(b)** 2D surface, **(c)** Streamline Plot **(d)** Polar Plot, of $\Xi_{15}(x,t)$: $\lambda_0 = 0$, $\lambda_1 = 0.9$, $\lambda_2 = -0.1$, $\mu = 1$, $\sigma = -1$, $\rho = -1$, $\eta = 1$, $\omega = 0.5$, $v = 1.05$.

5.1 Solution by New Kudryashov method

To find the exact solution of Equation 2.6, first we find value of positive integer $N = 2$ and plugging the value of N in to Equation 5.1 then Equation 5.1 will become as follows:

$$\Xi(\xi) = l_0 + l_1 g(\xi) + l_2 g(\xi)^2. \tag{5.4}$$

By putting the value of Equation 5.4 and Equation 5.1 in Equation 2.6, we obtain the following set of algebraic equations by equating the coefficients of different power of $g(\xi)$ is equal to zero. The values of unknown constants are obtained.

Set 1:

$$\mu = -\frac{-v\omega\eta + \eta^2 - \omega^2}{4\ln}(B)^2\delta^2\omega^4, \quad l_0 = \frac{-v\omega\eta + \eta^2 - \omega^2}{\sigma\omega^2}, \quad l_1 = 0, \quad l_2 = -\frac{6ab\left(-v\omega\eta + \eta^2 - \omega^2\right)}{\sigma\omega^2}. \tag{5.5}$$

By putting Set 1 in Equation 5.5, we get the exact solutions as follows:

$$\Xi_1(\xi) = \frac{-v\omega\eta + \eta^2 - \omega^2}{\sigma\omega^2} - \frac{6ab\left(-v\omega\eta + \eta^2 - \omega^2\right)}{\sigma\omega^2\left(aB^{\delta\xi} + bB^{-\delta\xi}\right)^2}. \tag{5.6}$$

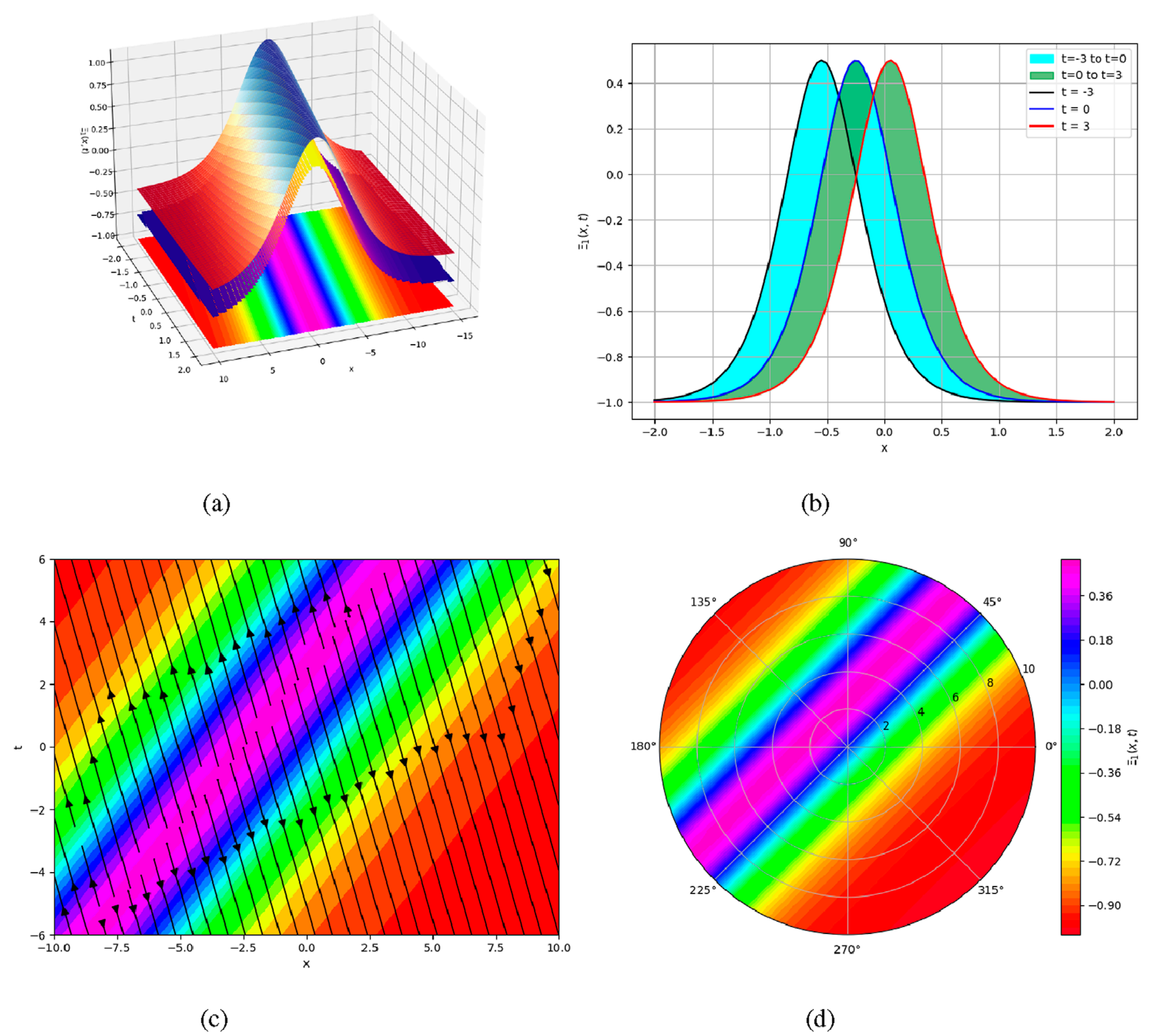

FIGURE 8
Graphical visualization of the derived solution of Equation 5.6 gives bright soliton such as **(a)** 3D surface, **(b)** 2D surface, **(c)** Streamline Plot **(d)** Polar Plot, of $\Xi_1(x,t)$: $\lambda_0 = 0$, $\lambda_1 = 0.9$, $\lambda_2 = -0.1$, $\mu = 1$, $\sigma = -1$, $\rho = -1$, $\eta = 1$, $\omega = 0.5$, $v = 1.05$.

Set 2:

$$v = \frac{4\ln(B)^2\delta^2\mu\omega^4 + \eta^2 - \omega^2}{\eta\omega}, l_0 = -\frac{4\delta^2\mu\ln(B)^2\omega^2}{\sigma}, l_1 = 0,$$
$$l_2 = \frac{24\ln(B)^2 ab\delta^2\mu\omega^2}{\sigma} \tag{5.7}$$

By putting Set 2 in Equation 5.7, we get the exact solutions as follows:

$$\Xi_2(\xi) = \frac{4\delta^2\mu\ln}{}(B)^2\omega^2\sigma + \frac{24\ln(B)^2 ab\delta^2\mu\omega^2}{\sigma\left(aB^{\delta\xi} + bB^{-\delta\xi}\right)^2}. \tag{5.8}$$

6 Stability analysis

In this section, we will discuss the stability of Equation 1.2. Consider a perturbed solution of Equation 1.2 has the form [57, 58].

$$\Xi(x,t) = P + \lambda U(x,t). \tag{6.1}$$

For any constant value of P, it is obvious that Equation 1.2 possesses a stable solution. U is the function of x,t, and λ is a real constant. By Inserting Equation 6.1 in Equation 1.2, we obtain the following result

$$\lambda U_{tt} - \sigma\lambda^2 U_{xx}^2 - \mu\lambda U_{xxxx} - v\lambda U_{xt} - \lambda U_{xx} = 0. \tag{6.2}$$

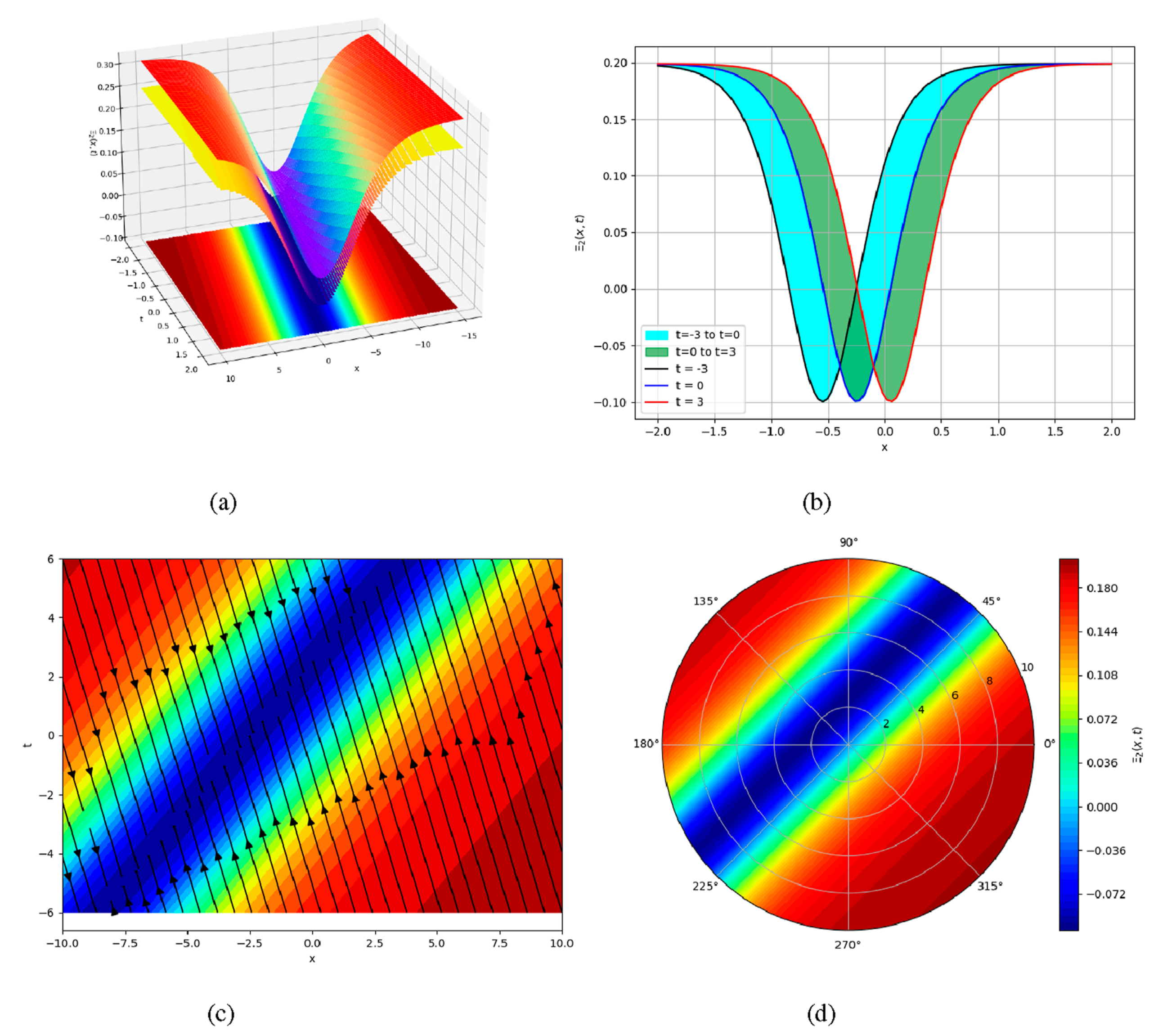

FIGURE 9
Graphical visualization of the derived solution of Equation 5.8 gives dark soliton such as **(a)** 3D surface, **(b)** 2D surface, **(c)** Streamline Plot **(d)** Polar Plot, of $\Xi_2(x,t)$: $\lambda_0 = 0$, $\lambda_1 = 0.9$, $\lambda_2 = -0.1$, $\mu = 1$, $\sigma = -1$, $\rho = -1$, $\eta = 1$, $\omega = 0.5$, $v = 1.05$.

Linearized Equation 6.2.

$$\lambda U_{tt} - \mu\lambda U_{xxxx} - v\lambda U_{xt} - \lambda U_{xx} = 0. \tag{6.3}$$

Suppose that Equation 6.3 has the solution of the from

$$U(x,t) = e^{\iota(mx-st)}. \tag{6.4}$$

Here, m represents the normalized wave numbers, and s represents the dispersion relation. By inserting Equation 6.4 into Equation 6.3, the following result is obtained

$$\left.\begin{aligned} s(m) &= \mu m^4 - m^2. \\ s(m) &= -m\theta - \mu m^4 + m^2. \end{aligned}\right\} \tag{6.5}$$

Now we'll look at the dispersed characteristics shown in Equation 6.5. The dispersion is stable if the real component of Equation 6.5 is negative for all m values. If it is positive, the dispersion is unstable. If it is zero, the dispersion is minimal.

7 Graphical representation and discussion

The graphical solutions produced using the Modified Sub-Equation, Generalized Arnous, and Kudryashov method to illustrate the presence of a wide range of soliton solutions within the framework of IBWWE. These visualizations also demonstrate how key parameters affect the wave behavior. Specifically, increasing the dispersion coefficient μ leads to sharper and narrower wave fronts, reflecting the intensification of dispersive mechanisms. Similarly, a higher nonlinearity parameter σ yields increased amplitude

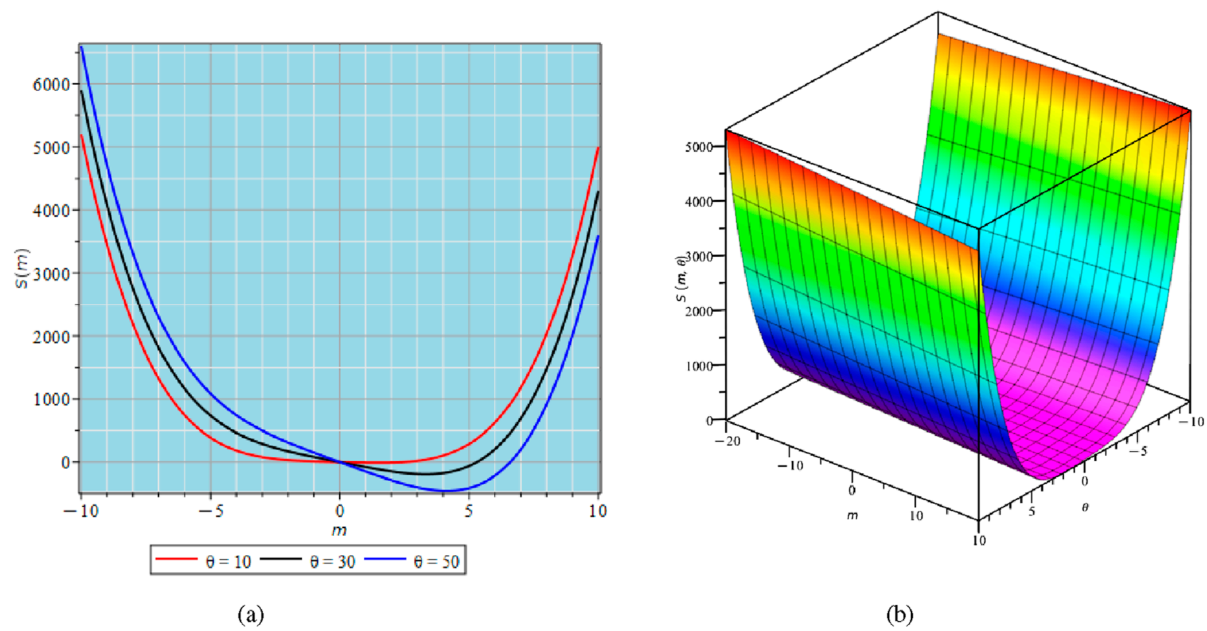

FIGURE 10
Stability analysis of system (6.5) with $\mu = 0.5$, m = −10,10, θ = −20,20. **(a)** 2D curve; **(b)** 3D surface.

and steepness, highlighting enhanced nonlinear interactions. The parameter ν plays a critical role in shaping the symmetry and phase behavior of the solutions the solution, sometimes introducing asymmetry or a deformed wave shape. These findings suggest that adjusting the model parameters allows control over wave localization, structural properties, and stability, offering practical insight into physical systems modeled by the IBWWE. The pictorial appearance of the solutions produced is investigated in this section. Specific values are supplied to the unknown constants to construct 3D and 2D graphs of the resulting solutions. The figures depicted in part (a) reflect a 3D plot, while part (b) represents the 2D line graph of the solutions, part (c) displays the Contour graph, and part (d) depicts the Polar plot. In Figure 1, the wave solution is visualized through 3D surfaces, 2D profiles, and contour maps under the parameter configuration $\Xi_{01}(x,t){:}\rho = 1, \theta = 0.2, \mu = 1, \omega = 0.3, \beta_2 = 1, \sigma = 1, \eta = 1, A = 0.5$, with the phase variable defined as $\xi = \omega x - \eta t$. The plots are generated for time slices $t = -1, 0, 1$. Figure 2 presents the wave evolution corresponding to a dark solitary structure under the same parameter configuration $\Xi_{02}(x,t)$, where the solution is illustrated through 3D plots, 2D line profiles, and contour maps for $t = -3, 0, 3$. In Figure 3, the bright solitary wave behavior is captured using the parameters $\Xi_{01}(x,t){:}\lambda_0 = 0, \lambda_1 = 1, \lambda_2 = 2, \mu = 2, \sigma = 1, \rho = 0.8, \eta = 0.5, \omega = 1, \nu = -8$, with $\xi = \omega x - \eta t$, and evaluated over the time domain $t = -5, 0, 5$. Figure 4 displays a dark-bright solitary wave structure governed by the constants $\Xi_{04}(x,t){:}\ \lambda_0 = 0.005, \lambda_1 = -0.1, \lambda_2 = 0.5, \mu = 2, \sigma = -2.5, \rho = 1, \eta = 0.5, \omega = 0.5, \nu = 0.56$, with $\xi = \omega x - \eta t$. The visual representation is provided for $t = -5, 0, 5$. In Figure 5, the anti-kink solitary wave is visualized using $\Xi_{06}(x,t){:}\lambda_0 = 0.001, \lambda_1 = -0.08, \lambda_2 = 1.2, \mu = 2, \sigma = -2.5, \rho = 2, \eta = 2, \omega = 1.4, \nu = 0.72 - 0.65i$, with $\xi = \omega x - \eta t$. The plots correspond to time levels $t = -3, 0, 3$. Figure 6 illustrates the bright solitary wave pattern for $\Xi_{14}(x,t){:}\lambda_0 = 0, \lambda_1 = 0.5, \lambda_2 = -0.5, \mu = 2, \sigma = 1, \rho = -1.5, \eta = 1, \omega = 0.5, \nu = 1$, with the phase $\xi = \omega x - \eta t$ and plots evaluated for $t = -3, 0, 3$. In Figure 7, the solution evolves under the parametric structure $\Xi_{15}(x,t){:}\lambda_0 = 0, \lambda_1 = 0.9, \lambda_2 = -0.1, \mu = 1, \sigma = -1, \rho = -1, \eta = 1, \omega = 0.5, \nu = 1.05$, with $\xi = \omega x - \eta t$. The visualization is provided for time slices $t = -1, 0, 1$. Figure 8 depicts a bright solitary wave structure governed by $\Xi_1(x,t){:}\lambda_0 = 0, \lambda_1 = 0.9, \lambda_2 = -0.1, \mu = 1, \sigma = -1, \rho = -1, \eta = 1, \omega = 0.5, \nu = 1.05$, with $\xi = \omega x - \eta t$, and evaluated at $t = -3, 0, 3$. In Figure 9, the dark solitary wave pattern is illustrated for $\Xi_2(x,t){:}\lambda_0 = 0, \lambda_1 = 0.9, \lambda_2 = -0.1, \mu = 1, \sigma = -1, \rho = -1, \eta = 1, \omega = 0.5, \nu = 1.05$, using the same phase $\xi = \omega x - \eta t$. The solution behavior is shown for time levels $t = -3, 0, 7$. Finally, Figure 10 provides the 3D surface and 2D projection visualizations reflecting the stability features of the system described by Equation 6.5, evaluated under the parameters $\mu = 0.5$, $m \in [-10, 10]$, and $\theta \in [-20, 20]$.

The bright soliton solution depicted in Figure 2 aligns well with theoretical expectations described in earlier studies of Boussinesq-type equations [53, 59]. As observed, increasing the dispersion parameter μ results in a narrowing of the soliton width and a sharper peak, which is consistent with the classical behavior of higher-order dispersive wave models [51]. Moreover, a rise in the nonlinear coefficient σ amplifies the soliton amplitude, supporting the expected balance between nonlinearity and dispersion.

In summary, the soliton profiles obtained in this work exhibit a broad range of wave behaviors, including bright, dark, anti-kink, periodic, and compound forms, which can be effectively modulated by tuning the model parameters. In contrast to conventional approaches such as the Hirota bilinear method, Exp-function method, or Lie symmetry techniques, which tend to yield classical solutions, the combined application of the Generalized

Arnous Method, Modified Sub-Equation Method, and Kudryashov Method facilitates the systematic construction of more intricate and previously unreported wave structures. Furthermore, the inclusion of graphical visualization and linear stability analysis provides further validation of the physical relevance and reliability of the solutions. These outcomes emphasize the utility of the proposed framework as a powerful analytical framework for solving higher-order nonlinear dispersive equations pertinent to fluid dynamics, coastal engineering, and nonlinear optics.

The proposed symbolic techniques, the Generalized Arnous Method, Modified Sub-Equation Method, and New Kudryashov Method, offer a computationally efficient framework for solving nonlinear PDEs. These methods transform the original equation into a solvable algebraic system using traveling wave transformations and a closed-form ansatz. The resulting complexity is polynomial in terms of symbolic manipulation steps, making them significantly faster and more tractable than numerical methods such as finite difference or spectral schemes, which require iterative time-stepping and grid refinement. In comparison with symbolic methods like the Hirota bilinear method or Riccati/ϕ^6 expansions, the proposed techniques provide greater generality in solution form, reduced reliance on fixed trial functions, and easier implementation in platforms such as Maple or Mathematica. These features collectively make the proposed methods both analytically powerful and computationally lightweight.

8 Conclusion

In this research, we applied the Generalized Arnous technique, plus the Novel Kudryashov and Modified Sub-Equation methods, to achieve accurate solutions for the fourth-order Boussinesq water wave equation which is an important tool for the investigation of nonlinear phenomena in various waves and shallow water phenomena in fluid dynamics, such as diffraction, refraction, weak non-linearity, and shoaling. It was important to apply a special wave transformation method to change the original NLPDE into a NODE to accomplish this aim. Notably, these methodologies produced a diverse variety of soliton solutions, including periodic (repeating waveforms that maintain their shape and speed while traveling, combining features of both solitary and periodic waves), bright (localized areas of elevated intensity, when the wave amplitude attains its zenith, resulting in peaks or humps within the wave profile.), dark (low-intensity areas inside a high-intensity backdrop. In these places, the wave amplitude falls below the background level, resulting in troughs or depressions in the wave profile.), dark-bright, bright-dark solitons. For a thorough comprehension of the physical processes inherent in the fourth-order BE, we graphically portrayed chosen solutions by assigning parameter values in 3*D*-surface graphs, 2*D*-line graphs, and contour and Polar plots, according to particular limitations. These graphical representations aid in deepening our knowledge of the various soliton structures originating from the equation. Additionally, we underlined the usefulness and potency of the Generalized Arnous method, the New Kudryashov, and the Modified Sub-Equation strategies in discovering soliton solutions for NLPDEs. The discovered solutions contribute greatly to expanding our grasp of the nonlinear dynamics regulating the propagation of water solitons in engineering and physical sciences. This paper tries to give helpful insights for scientists and researchers aiming to enhance their experimental activities. Moreover, there exists a possibility for widening the scope of this study by including concerns of lump interactions, researching multi-soliton situations, and analyzing the dynamics of rogue wave breathers. Such additions might improve the practical application and relevance of the research. The distinctiveness of this study lies in the unified application of three analytical techniques to systematically investigate the complex soliton dynamics in the IBWWE, yielding new solutions such as bright-dark and anti-kink solitons. The detailed stability analysis and graphical illustrations, supported by reproducible resources, extend the application of this work to both theoretical studies and practical applications in fluid dynamics, in coastal, optical, and plasma environments.

Data availability statement

The original contributions presented in the study are included in the article/Supplementary Material, further inquiries can be directed to the corresponding author.

Author contributions

KF: Supervision, Writing – review and editing. FA: Supervision, Writing – review and editing. ZL: Writing – review and editing, Supervision. EH: Software, Writing – review and editing, Writing – original draft.

Funding

The author(s) declare that financial support was received for the research and/or publication of this article. This work was supported and funded by the Deanship of Scientific Research at Imam Mohammad Ibn Saud Islamic University (IMSIU) (grant number IMSIU-DDRSP2503).

Conflict of interest

The authors declare that the research was conducted in the absence of any commercial or financial relationships that could be construed as a potential conflict of interest.

The handling editor WM declared a past co-authorship with the author(s) ZL and EH.

Generative AI statement

The author(s) declare that no Generative AI was used in the creation of this manuscript.

Any alternative text (alt text) provided alongside figures in this article has been generated by Frontiers with the support of artificial intelligence and reasonable efforts have been made to ensure accuracy, including review by the authors wherever possible. If you identify any issues, please contact us.

Publisher's note

All claims expressed in this article are solely those of the authors and do not necessarily represent those of their affiliated organizations, or those of the publisher, the editors and the reviewers. Any product that may be evaluated in this article, or claim that may be made by its manufacturer, is not guaranteed or endorsed by the publisher.

References

1. Boussinesq J. Theory of liquid intumescence called solitary or translational wave propagating in a rectangular channel. *CR Acad Sci Paris* (2021) 72(755-759):1871.

2. Tian S. Lie symmetry analysis, conservation laws and solitary wave solutions to a fourth-order nonlinear generalized Boussinesq water wave equation. *Appl Mathematics Lett* (2020) 100:106056. doi:10.1016/j.aml.2019.106056

3. Singh S, Kaur L, Sakkaravarthi K, Sakthivel R, Murugesan K. Dynamics of higher-order bright and dark rogue waves in a new (2+ 1)-dimensional integrable Boussinesq model. *Physica Scripta* (2020) 95(11):115213. doi:10.1088/1402-4896/abbca0

4. Wazwaz A, Kaur L. New integrable Boussinesq equations of distinct dimensions with diverse variety of soliton solutions. *Nonlinear Dyn* (2019) 97:83–94. doi:10.1007/s11071-019-04955-1

5. Wang P, Liu Z, Fang K, Sun J, Gou D. High-order Boussinesq equations for water wave propagation in porous media. *Water* (2023) 15(22):3900. doi:10.3390/w15223900

6. Fan S, Sun T, Liu P, Yu D. Travelling wave solutions of nonlinear evolution problem arising in mathematical physics through-expansion scheme. *Math Probl Eng* 2022(1):6557949–2022.

7. Pu JC, Chen Y. Nonlocal symmetries, Bäcklund transformation and interaction solutions for the integrable Boussinesq equation. *Mod Phys Lett B* (2020) 34(26):2050288. doi:10.1142/s0217984920502887

8. Kumar S, Malik S, Rezazadeh H, Akinyemi L. The integrable Boussinesq equation and it's breather, lump and soliton solutions. *Nonlinear Dyn* (2022) 107:2703–16. doi:10.1007/s11071-021-07076-w

9. Mitsotakis DE. Boussinesq systems in two space dimensions over a variable bottom for the generation and propagation of tsunami waves. *Mathematics Comput Simulation* (2009) 80(4):860–73. doi:10.1016/j.matcom.2009.08.029

10. Kennedy AB, Chen Q, Kirby JT, Dalrymple RA. Boussinesq modeling of wave transformation, breaking, and runup. i: 1d. *J Waterway, Port, Coastal, Ocean Eng* (2000) 126(1):39–47. doi:10.1061/(asce)0733-950x(2000)126:1(39)

11. Madsen PA, Sørensen OR. Extension of the Boussinesq equations to include wave propagation in deeper water and wave-ship interaction in shallow water. In: *Coastal engineering 1990, proceedings of the 22nd International Conference*. Delft, Netherlands: ASCE (1993). p. 3112–25.

12. Denys D, Henrik K. Boussinesq modeling of surface waves due to underwater landslides. *Nonlinear Process Geophys* (2013) 20(3):267–85.

13. Clarkson PA, Dowie E. Applications of soliton theory to shallow water equations. *Stud Appl Mathematics* (2016) 137(3):322–45.

14. Raymond G, Abdullah SK, Zaher AB, Julien MHB, Zia Ur R. Non-linear plasma wave dynamics: investigating chaos in dynamical systems. *Mathematics* (2024) 12(18):2958. doi:10.3390/math12182958

15. Akram T, Iqbal A, Ali A, Sarwar S. *Numerical Simulation of Wave Disturbances of the High Order Boussinesq Equations* (2024). doi:10.2139/ssrn.4769424

16. Sebogodi M, et al. Optical soliton dynamics modeled by integrable nonlinear equations. *Results Phys* (2023) 51:106646.

17. Lederer F, Stegeman GI, Christodoulides DN, Assanto G, Segev M, Silberberg Y. Discrete solitons in optics. *Phys Rep* (2008) 463(1-3):1–126. doi:10.1016/j.physrep.2008.04.004

18. Sommerfeld A. *Partial differential equations in physics*. Academic Press (1949).

19. Ames WF. *Nonlinear partial differential equations in engineering*. Academic Press (1965).

20. Islam SR, Khan K, Akbar MA. Optical soliton solutions, bifurcation, and stability analysis of the Chen-Lee-Liu model. *Results Phys* (2023) 51:106620. doi:10.1016/j.rinp.2023.106620

21. Attia RA, Xia Y, Zhang X, Khater MM. Analytical and numerical investigation of soliton wave solutions in the fifth-order KdV equation within the KdV-kP framework. *Results Phys* (2023) 51:106646. doi:10.1016/j.rinp.2023.106646

22. Khater MM. Physics of crystal lattices and plasma; analytical and numerical simulations of the Gilson–Pickering equation. *Results Phys* (2023) 44:106193. doi:10.1016/j.rinp.2022.106193

23. Murad MAS, Mahmood SS, Emadifar H, Mohammed WW, Ahmed KK. Optical soliton solution for dual-mode time-fractional nonlinear Schrödinger equation by generalized exponential rational function method. *Results Eng* (2025) 27:105591. doi:10.1016/j.rineng.2025.105591

24. Ozdemir N, Secer A, Ozisik M, Bayram M. Optical solitons for the dispersive Schrödinger–Hirota equation in the presence of spatiotemporal dispersion with parabolic law. *The Eur Phys J Plus* (2023) 138(6):1–10.

25. Khater MM. Abundant and accurate computational wave structures of the nonlinear fractional biological population model. *Int J Mod Phys B* (2023) 37(18):2350176. doi:10.1142/s021797922350176x

26. Karamali G, Dehghan M, Abbaszadeh M. Numerical solution of a time-fractional PDE in the electroanalytical chemistry by a local meshless method. *Eng Comput* (2019) 35:87–100. doi:10.1007/s00366-018-0585-7

27. Zauderer E. *Partial differential equations of applied mathematics*. John Wiley and Sons (2011).

28. Tufillaro N. An experimental approach to nonlinear dynamics and chaos. *ScienceOpen Preprints* (2024).

29. Chowdhury MA, Miah MM, Rasid MM, Rehman S, Borhan J, Wazwaz A, et al. Further quality analytical investigation on soliton solutions of some nonlinear PDEs with analyses: bifurcation, sensitivity, and chaotic phenomena. *Alexandria Eng J* (2024) 103:74–87. doi:10.1016/j.aej.2024.05.096

30. Hussain E, Younas U, Tapdigoglu R, Garayev M. Exploring bifurcation, quasi-periodic patterns, and wave dynamics in an extended calogero-bogoyavlenskii-schiff model with sensitivity analysis. *Int J Theor Phys* (2025) 64(5):146. doi:10.1007/s10773-025-06008-3

31. Iqbal I, Boulaaras SM, Althobaiti S, Althobaiti A, Rehman HU. Exploring soliton dynamics in the nonlinear Helmholtz equation: bifurcation, chaotic behavior, multistability, and sensitivity analysis. *Nonlinear Dyn* (2025) 113:16933–54. doi:10.1007/s11071-025-10961-3

32. Rafiq MN, Rafiq MH, Alsaud H. New insights into the diversity of stochastic solutions and dynamical analysis for the complex cubic NLSE with δ-potential through Brownian process. *Commun Theor Phys* (2025) 77:075001. doi:10.1088/1572-9494/adaddd

33. Tariq MM, Riaz MB, ur Rehman MA, Dilawaiz . Unraveling the complexity of solitary waves in the Klein-Fock-Gordon equation: dynamical insights into bifurcation and Chaos analysis. *Model Earth Syst Environ* (2025) 11(1):51–17. doi:10.1007/s40808-024-02249-z

34. Kopçasız B, Nur Kaya Sağlam F. Exploration of soliton solutions for the Kaup–Newell model using two integration schemes in mathematical physics. *Math Methods Appl Sci* (2025).

35. Sadaf M, Arshed S, Akram G, Ahmad M, Abualnaja KM. Solitary dynamics of the Caudrey–Dodd–Gibbon equation using unified method. *Opt Quan Electronics* (2025) 57(1):21–2. doi:10.1007/s11082-024-07899-y

36. Arafat SMY, Islam SMR. Bifurcation analysis and soliton structures of the truncated M-fractional Kuralay-II equation with two analytical techniques. *Alexandria Eng J* (2024) 105:70–87. doi:10.1016/j.aej.2024.06.079

37. Gu C, Hu H, Zhou Z. *Darboux transformations in integrable systems: theory and their applications to geometry*. Springer Science and Business Media (2004).

38. He J, Wu X. Exp-function method for nonlinear wave equations. *Chaos, Solitons and Fractals* (2006) 30(3):700–8. doi:10.1016/j.chaos.2006.03.20

39. Islam MS, Khan K, Arnous AH. Generalized Kudryashov method for solving some (3+ 1)-dimensional nonlinear evolution equations. *New Trends Math Sci* (2015) 3(3):46.

40. Gurefe Y, Misirli E, Sonmezoglu A, Ekici M. Extended trial equation method to generalized nonlinear partial differential equations. *Appl Mathematics Comput* (2013) 219(10):5253–60. doi:10.1016/j.amc.2012.11.046

41. Hietarinta J. Introduction to the Hirota bilinear method. In: *Integrability of nonlinear systems: Proceedings of the CIMPA School Pondicherry University, India, 8–26 January 1996*. Springer (2007). p. 95–103.

42. Yan Z. The extended Jacobian elliptic function expansion method and its application in the generalized Hirota–Satsuma coupled KdV system. *Chaos, Solitons and Fractals* (2003) 15(3):575–83. doi:10.1016/s0960-0779(02)00145-5

43. Mirhosseini-Alizamini SM, Rezazadeh H, Eslami M, Mirzazadeh M, Korkmaz A. New extended direct algebraic method for the Tzitzica type evolution equations arising in nonlinear optics. *Comput Methods Differential Equations* (2020) 8(1):28–53.

44. Yiasir Arafat SM, Fatema K, Rayhanul Islam SM, Islam ME, Ali Akbar M, Osman MS. The mathematical and wave profile analysis of the Maccari system in nonlinear

physical phenomena. *Opt Quan Electronics* (2023) 55(2):136. doi:10.1007/s11082-022-04391-3

45. El-Wakil S, Abdou M. The extended Fan sub-equation method and its applications for a class of nonlinear evolution equations. *Chaos, Solitons and Fractals* (2008) 36(2):343–53. doi:10.1016/j.chaos.2006.06.065

46. Hussain E, Tedjani AH, Farooq K, Beenish . Modeling and exploration of localized wave phenomena in optical fibers using the generalized Kundu–Eckhaus equation for Femtosecond pulse transmission. *Axioms* (2025) 14(7):513. doi:10.3390/axioms14070513

47. Khizar F, Ali HT, Zhao L, Ejaz H. Soliton dynamics of the nonlinear kodama equation with M-truncated derivative via two innovative schemes: the generalized arnous method and the kudryashov method. *Fractal and Fractional* (2025) 9(7):436. doi:10.3390/fractalfract907436

48. Murad MAS, Ismael HF, Hamasalh FK, Shah NA, Eldin SM. Optical soliton solutions for time-fractional Ginzburg–Landau equation by a modified sub-equation method. *Results Phys* (2023) 53:106950. doi:10.1016/j.rinp.2023.106950

49. Khizar F, Ejaz H, Usman Y, Mukalazi H, Khalaf TM, Mutlib A, et al. Exploring the wave's structures to the nonlinear coupled system arising in surface geometry. *Scientific Rep* (2025) 15:11624. doi:10.1038/s41598-024-84657-w

50. Drazin PG, Johnson RS. *Solitons: an introduction*. Cambridge University Press (1989).

51. Ablowitz MJ, Segur H. *Solitons and the Inverse Scattering transform*. Philadelphia, PA: SIAM (1981).

52. Scott AC, Chu FYF, McLaughlin DW *The soliton: a new Concept in applied science*, Vol. 61. IEEE (1973).

53. Wazwaz AM, Kaur D. Integrable Boussinesq-type equations with multiple soliton solutions and Painlevé analysis. *Results Phys* (2019) 15:102691.

54. He J-H, Wu X-H. Exp-function method for nonlinear wave equations. *Chaos, Solitons and Fractals* (2006) 30(3):700–8. doi:10.1016/j.chaos.2006.03.020

55. Kudryashov NA. Exact soliton solutions of the generalized evolution equation of wave dynamics. *J Appl Mathematics Mech* (2005) 69(3):405–9.

56. Raees N, Mahmood I, Hussain E, Younas U, Elansary HO, Mumtaz S. Dynamics of optical solitons and sensitivity analysis in fiber optics. *Phys Lett A* (2024) 528:130031. doi:10.1016/j.physleta.2024.130031

57. Mahmood I, Hussain E, Mahmood A, Anjum A, Shah S. Optical soliton propagation in the Benjamin–Bona–Mahoney–Peregrine equation using two analytical schemes. *Optik* (2023) 287:171099. doi:10.1016/j.ijleo.2023.171099

58. Hussain E, Li Z, Shah SAA, Az-Zo'bi EA, Hussien M. Dynamics study of stability analysis, sensitivity insights and precise soliton solutions of the nonlinear (sto)-burger equation. *Opt Quan Electronics* (2023) 55(14):1274. doi:10.1007/s11082-023-05588-w

59. Khater HA, Selim MM, Zayed ME, Elgarayhi A. New complex soliton structures of the fractional extended Boussinesq equation. *Mathematics Comput Simulation* (2023).